BIOCHEMISTRY
including biophysical chemistry & molecular biology

Article

pubs.acs.org/biochemistry

Photoinitiated Electron Transfer within the *Paracoccus denitrificans* Cytochrome bc_1 Complex: Mobility of the Iron–Sulfur Protein Is Modulated by the Occupant of the Q_o Site

Jeffrey Havens,[†,§] Michela Castellani,[‡,§,∥] Thomas Kleinschroth,[‡,⊥] Bernd Ludwig,[‡] Bill Durham,[†] and Francis Millett*[,†]

[†]Department of Chemistry and Biochemistry, University of Arkansas, Fayetteville, Arkansas 72701, United States

[‡]Institute of Biochemistry, Molecular Genetics, Goethe University and Cluster of Excellence Macromolecular Complexes, Frankfurt am Main, D-60438 Frankfurt am Main, Germany

Supporting Information

ABSTRACT: Domain rotation of the Rieske iron–sulfur protein (ISP) between the cytochrome (cyt) *b* and cyt c_1 redox centers plays a key role in the mechanism of the cyt bc_1 complex. Electron transfer within the cyt bc_1 complex of *Paracoccus denitrificans* was studied using a ruthenium dimer to rapidly photo-oxidize cyt c_1 within 1 μs and initiate the reaction. In the absence of any added quinol or inhibitor of the bc_1 complex at pH 8.0, electron transfer from reduced ISP to cyt c_1 was biphasic with rate constants of k_{1f} = 6300 ± 3000 s^{-1} and k_{1s} = 640 ± 300 s^{-1} and amplitudes of 10 ± 3% and 16 ± 4% of the total amount of cyt c_1 photooxidized. Upon addition of any of the P_m type inhibitors MOA-stilbene, myxothiazol, or azoxystrobin to cyt bc_1 in the absence of quinol, the total amplitude increased 2-fold, consistent with a decrease in redox potential of the ISP. In addition, the relative amplitude of the fast phase increased significantly, consistent with a change in the dynamics of the ISP domain rotation. In contrast, addition of the P_f type inhibitors JG-144 and famoxadone decreased the rate constant k_{1f} by 5–10-fold and increased the amplitude over 2-fold. Addition of quinol substrate in the absence of inhibitors led to a 2-fold increase in the amplitude of the k_{1f} phase. The effect of QH_2 on the kinetics of electron transfer from reduced ISP to cyt c_1 was thus similar to that of the P_m inhibitors and very different from that of the P_f inhibitors. The current results indicate that the species occupying the Q_o site has a significant conformational influence on the dynamics of the ISP domain rotation.

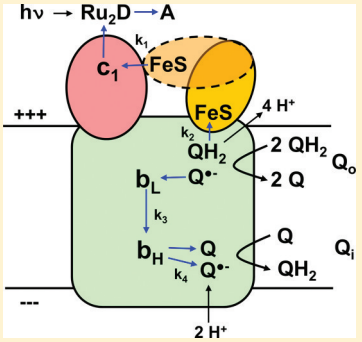

Cytochrome bc_1 is an integral membrane protein of the electron transfer chains of mitochondria and the plasma membranes of oxygenic prokaryotes.[1,2] The cyt bc_1 complex of the soil bacterium *Paracoccus denitrificans* has a number of unusual features.[3] It contains just three subunits: the *b* subunit containing heme b_L and heme b_H, the Rieske iron–sulfur protein (ISP), and cyt c_1. Hydropathy and sequence analysis studies have indicated that cyt c_1 has a tripartite domain structure consisting of a C-terminal membrane anchor, a periplasmically oriented core domain containing the covalently attached heme *c*, and a unique N-terminal acidic domain of 150 amino acids. The acidic domain may be analogous to the small acidic subunits of eukaryotic cyt bc_1, including the hinge protein of bovine cyt bc_1 and subunit 6 of yeast cyt bc_1.[4,5] Another unusual feature of *P. denitrificans* cyt bc_1 is that mass spectrometry studies have shown that it has a quaternary structure described as a "dimer of dimers" rather than the dimeric structure found in other cyt bc_1 complexes.[6]

Cyt bc_1 from all species is thought to function as described by the Q-cycle, in which four protons are translocated to the positive (P) side of the membrane as two electrons are transferred from ubiquinol to cyt *c*.[1,2,7,8] A key step in the Q-cycle is the bifurcation of two electrons from quinol in the Q_o site to the high and low potential chains.[7,8] The first electron is transferred from quinol to the ISP and then to cyt c_1 and cyt *c*. The second electron is transferred across the membrane via hemes b_L and b_H to ultimately reduce quinone bound at the Q_i site.

X-ray crystallographic studies have shown that the orientation of the ISP is affected by inhibitors in the Q_o site.[9−12] Structures with stigmatellin bound at the Q_o site reveal that the ISP is oriented close to the *b* subunit (called the *b*-state) and is stabilized by a hydrogen bond between His^{161} (a ligand of the [2Fe2S] cluster) and a carbonyl group of the inhibitor.[12−16] In contrast, the Q_o site inhibitor myxothiazol binds within the Q_o pocket in a position more proximal to heme b_L without bonding contact to the ISP and appears to release the ISP from the *b* state to a disordered state as evidenced by decreased anomalous [2Fe2S] peak heights.[12,17] On the basis of the effects of Q_o site (P site) inhibitors on the observed position of the ISP, they have recently been categorized as either P_m, to denote a mobile ISP, or P_f, to

Received: March 26, 2011
Revised: October 22, 2011
Published: October 25, 2011

denote the ISP fixed in the *b* state.[14] The P_m type inhibitors include methoxyacrylate type inhibitors such as MOA-stilbene, azoxystrobin, and myxothiazol. P_f type inhibitors include stigmatellin, UHDBT, famoxadone, and JG-144. These structural studies have led to the proposal that the ISP functions as a mobile shuttle, first binding in the *b* state to accept an electron from quinol in the Q_o site and then rotating by 57° to the c_1 state where it transfers an electron to cyt c_1.[10,11] The mobile shuttle mechanism has been supported by a number of mutational, EPR, and cross-linking studies.[18−32]

The photoactive ruthenium complex, Ru_2D, was developed to measure the rate constant for electron transfer between the ISP and cyt c_1, which is too rapid to measure by other techniques.[18,26,33−36] Ru_2D, with a net charge of 4+, binds to the negatively charged domain on cyt c_1. Laser flash activation of Ru_2D to the metal-to-ligand excited state results in oxidation of cyt c_1 within 1 μs in the presence of a sacrificial electron acceptor. The subsequent electron transfer reaction from the reduced ISP to cyt c_1 is then measured by transient absorbance changes in the c_1 heme. Flash photolysis studies of *R. sphaeroides* and bovine cytochromes bc_1 using Ru_2D have established that the rate constant for electron transfer between the ISP and cyt c_1 is "conformationally gated" by the rotation of the ISP from the *b* state to the c_1 state.[26] The ruthenium photooxidation method is thus a unique way to study the dynamics of ISP domain movement and complement the structural and EPR studies.

In this study the rapid electron transfer reactions within the cyt bc_1 complex of *P. den* are reported for the first time. A number of different P_f and P_m Q_o site inhibitors are found to have significant effects on the kinetics of the electron transfer reaction from the ISP to heme c_1. The P_m type inhibitors significantly increase the extent of the electron transfer reaction from the ISP to cyt c_1. The presence of the quinol substrate also significantly increases the extent of the initial electron transfer reaction from ISP to heme c_1, suggesting that quinol binding to the bc_1 complex also causes conformational changes in the *b* subunit which may regulate the mobility of the ISP.

MATERIALS AND METHODS

Purification of Cytochrome bc_1 from *P. den*. Membrane aliquots were thawed, and the protein concentration was adjusted to 35 mg/mL. Membranes were solubilized upon addition of Pefabloc SC, 100 μM final concentration, one volume of solubilization buffer (100 mM MES/NaOH pH 6, 600 mM sucrose, 2.4 M NaCl), and dodecylmaltoside (DDM) in a weight ratio 1.2:1 to the total protein. The solution was then stirred 1 h at 4 °C. The solubilizate was then centrifuged (Beckmann Ti 45 rotor, 35 000 rpm, 1 h at 4 °C), and the supernatant, which now had a NaCl concentration of 600 mM, was diluted to 350 mM NaCl and filtered using a paper filter. The ion exchange column (DEAE-Sepharose CL-6B, ca. 250 mL, FPLC Pharmacia LKB) was equilibrated with 4 column volumes (CV) equilibration buffer (50 mM MES/NaOH pH 6, 350 mM NaCl) and 2 CV low salt buffer (50 mM MES/NaOH pH 6, 350 mM NaCl, 0.02% DDM). The solubilizate was applied to the column with a flow rate of 3.5 mL/min and afterward washed with 1 CV of low salt buffer. All proteins not tightly binding to the column were washed away. The bc_1 complex was eluted with a 6 CV NaCl gradient (350−600 mM NaCl, 50 mM MES/NaOH, pH 6, 0.02% DDM). The elution profile was recorded with a detector (Pharmacia Optical Unit UV-1, 280 nm) and a printer (Pharmacia Rec 102). The elution of the red fractions containing the bc_1 complex occurred at about 420−450 mM NaCl, and the fractions were analyzed spectroscopically and by SDS and Western Blot. The fractions containing pure protein were collected and concentrated by a factor of 150−200 (Satorius Vivaspin cutoff 100 kDa). The amount of endogenous quinone substrate in purified cyt bc_1 was determined by FTIR to be 1.92 ± 0.02 quinones per bc_1 monomer.

Flash Photolysis Experiments. Electron transfer reactions within *P. den* cyt bc_1 were studied following flash initiated oxidation of the c_1 heme by the binuclear ruthenium complex, Ru_2D. Transient absorbencies were detected following excitation of Ru_2D by a 480 nm light flash of less than 500 ns duration provided by a phase R model DL1400 flash lamp-pumped dye laser using coumarin LD 490. The detection system was as described previously by Heacock et al.[37] and had a response time of less than 200 ns. 5−10 transients were averaged to obtain the final transient signal. Solution reagents were contained in a 1 cm quartz microcuvette to a volume of 300 μL, typically buffered at pH 8.0 by 20 mM TRIS-HCl and additionally containing 5 mM of the sacrificial oxidant $[Co(NH_3)_5Cl]^{2+}$ and 0.02% DDM. For studies at pH 6, pH 7, and pH 9, 20 mM MES, 5 mM phosphate, and 20 mM borate buffers were used, respectively. Enzyme, ruthenium reagent, and substrate concentrations were typically 5 μM cyt bc_1, 20 μM Ru_2D, and 100 μM decylubiquinone, respectively. 2 mM succinate and 50 nM SCR were included in reactions with substrate to ensure sufficient reduction of the quinone. In order to further ensure full reduction of the high potential chain substituents, the redox mediators TMPD and ascorbate were added to 4 μM and 1 mM, respectively. All solutions were made anaerobic by an N_2 flush and appropriate use of septa and maintained at 10 °C by a VWR Scientific Model 1160A pump water bath flowing through an in-house-designed cell holder. All inhibitors, substrates, and redox mediators were purchased from Sigma-Aldrich and either made fresh or appropriately stored as concentrated stocks, except for JG-144 and MOAS, which were generously provided from the laboratories of Dr. Di Xia and Dr. Chang-An Yu, respectively. Transients were fitted either to the sum of two exponentials or to the Kohlrausch−Williams−Watts stretched exponential function:

$$A = A_1(1 - \exp(-kt)^{\beta})$$

where β is inversely related to the Levy distribution of rate constants, $0 < \beta < 1$, and k is the characteristic rate constant.[38] Data fitting was carried out by least-squares minimization using the Levenberg−Marquardt method in Sigma Plot. The zero-point in time was set at the very beginning of the transient reduction of cyt c_1 immediately after photooxidation of cyt c_1 by the laser flash was complete. In the figures, the zero point of the time axis is set at the beginning of the reductive transient, and the arrow shows the time of the laser flash. The error limits reported were obtained from at least five independent measurements.

RESULTS

Electron Transfer between the ISP and cyt c_1 in *P. den* cyt bc_1. Electron transfer within cyt bc_1 was studied using the ruthenium dimer Ru_2D to photo-oxidize cyt c_1 according to Scheme 1. A solution containing Ru_2D and wild-type cyt bc_1 was treated with ascorbate and TMPD to fully reduce cyt c_1 and [2Fe2S] under anaerobic conditions. Laser flash photolysis

Scheme 1

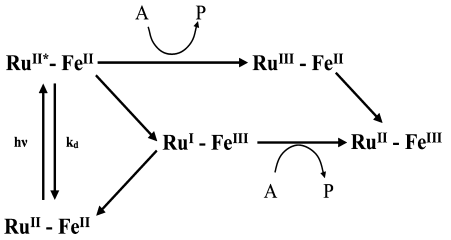

Scheme 2

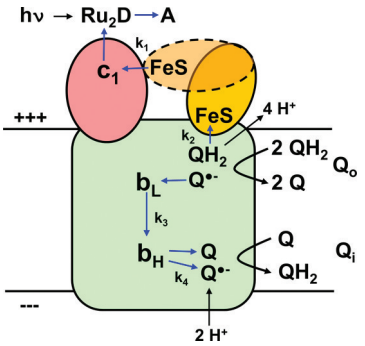

excited Ru_2D to the metal-to-ligand excited state, which rapidly oxidized cyt c_1 within 700 ns, as indicated by the rapid decrease in absorbance at 552 nm, the cyt c_1 α peak (Scheme 1, Figure 1a). The sacrificial oxidant $[Co(NH_3)_5Cl]^{2+}$ was present in solution to accept an electron from reduced Ru_2D (A in Schemes 1 and 2). The +4 charge on Ru_2D makes it highly selective for photooxidizing exposed redox centers in acidic protein surfaces.[18] The photooxidation of cyt c_1 was complete in the lifetime of the Ru_2D excited state, 630 ns,[18] with no contribution from a slower, second-order diffusion process (Supporting Information Figure 1). Ru_2D must be in direct contact with the heme edge of cyt c_1 or very close to it at the time of the flash to achieve electron transfer in this time period. The large redox potential of the Ru_2D(III/II) transition, +1.24 V, ensures that any Ru_2D(III) generated in solution by $[Co(NH_3)_5Cl]^{2+}$ would be

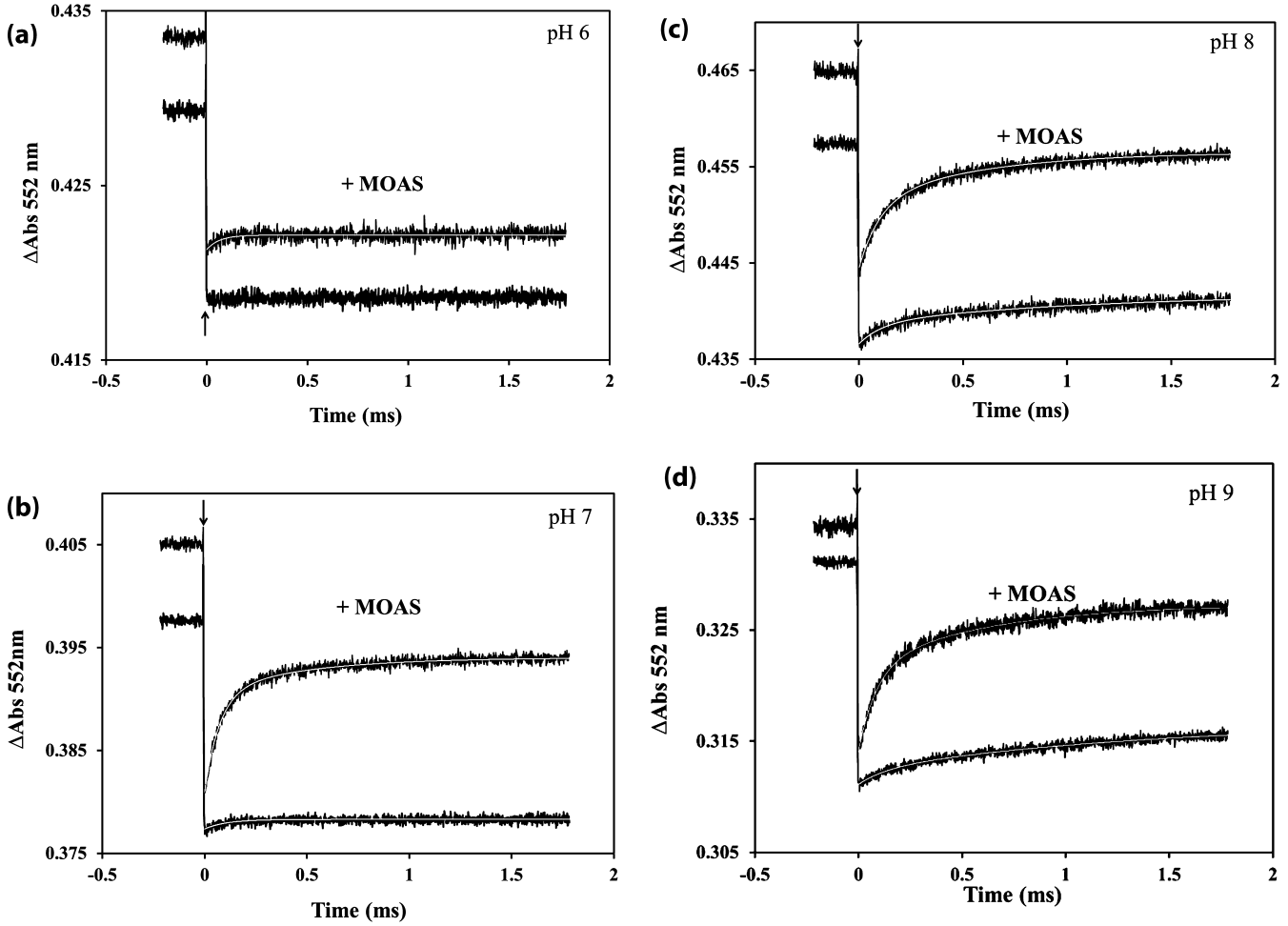

Figure 1. Effects of pH and MOAS on the kinetics of electron transfer between [2Fe2S] and cyt c_1. Approximately 5 μM cyt bc_1 was rapidly oxidized by 20 μM Ru_2D following a laser flash at the indicated pH. Solutions were buffered at pH 6 (a), pH, 7 (b), pH 8 (c), and pH 9 (d) by 20 mM MES, 5 mM phosphate, 20 mM TRIS-HCl, and 20 mM borate, respectively. 5 mM $[Co(NH_3)_5Cl]^{2+}$ was present to act as a sacrificial oxidant of excited state Ru_2D. Cyt c_1 and [2Fe2S] were reduced by 1 mM ascorbate and 4 μM TMPD. All solutions were purged with an N_2 flush and kept at 10 °C. The two transients in each figure correspond to before (lower transient) and after (upper transient) addition of 25 μM MOAS. The upper transient was offset relative to the lower. Transients were fit using either a single or sum of two exponential function represented by the single white line through each transient. The zero-point in time was set at the very beginning of the transient reduction of cyt c_1, and the arrow shows the time of the laser flash.

dx.doi.org/10.1021/bi200453r | *Biochemistry* 2011, 50, 10462–10472

rapidly reduced by ascorbate and other mediators, which are present in large excess over cyt bc_1. To study the role of the protein surface charge in photooxidation by Ru_2D, experiments were performed on horse cyt *c*, with a heme as exposed to solvent as that of cyt c_1, but with lysine residues surrounding the heme crevice. No detectable photo-oxidation of reduced horse cyt *c* by Ru_2D was detected under the same conditions as Figure 1a, even in the presence of 500 mM NaCl, which would shield any electrostatic repulsion of Ru_2D (Supporting Information Figure 2). The ISP has no acidic residues close to the [2Fe2S] center, but a number of basic residues (Supporting Information Figure 3). Moreover, the [2Fe2S] center is completely buried in the *b* state of the ISP and rather obstructed in the other states examined by X-ray crystallography. It is unlikely that Ru_2D would directly photooxidize [2Fe2S] in the ISP protein of cyt bc_1.

The extent of the electron transfer reaction from [2Fe2S] to cyt c_1 depends on the difference in redox potentials between the two redox centers, $\Delta E_0 = E_0(c_1) - E_0(\mathrm{FeS})$, which is dependent on pH.[39] Photoinduced electron transfer was therefore studied as a function of pH (Figure 1, Table 1).

Table 1. Effects of pH and MOAS on Electron Transfer between [2Fe2S] and cyt c_1 in *P. den* cyt bc_1[a]

pH	inhibitor	k_{1f} (s^{-1})	A_{1f} (%)	k_{1s} (s^{-1})	A_{1s} (%)
6	none	nd	nd	nd	nd
	MOAS	16000 ± 5000	5 ± 2	nd	nd
7	none	9300 ± 4000	5 ± 2	nd	nd
	MOAS	14000 ± 3000	40 ± 8	2100 ± 400	15 ± 3
8	none	6300 ± 3000	10 ± 3	640 ± 300	16 ± 4
	MOAS	9900 ± 2000	33 ± 7	1800 ± 400	26 ± 5
9	none	7500 ± 3000	6 ± 2	1000 ± 200	22 ± 4
	MOAS	11600 ± 2300	37 ± 7	1700 ± 400	29 ± 6

[a]Approximately 5 μM cyt bc_1 was rapidly oxidized by 20 μM Ru_2D following a laser flash at the indicated pH. Solutions were buffered at pH 6, pH, 7, pH 8, and pH 9 by 20 mM MES, 5 mM phosphate, 20 mM TRIS-HCl, and 20 mM borate, respectively. 5 mM $[Co(NH_3)_5Cl]^{2+}$ was present to act as a sacrificial oxidant of excited state Ru_2D. Cyt c_1 and [2Fe2S] were reduced by 1 mM ascorbate and 4 μM TMPD. 25 μM MOAS was added where indicated. All solutions were purged with an N_2 flush and kept at 10 °C. The rate constants k_{1f} and k_{1s} represent the fast and slower phases observed at 552 nm, respectively. A_{1f} and A_{1s} are the relative amplitudes of k_{1f} and k_{1s}, respectively, and represent the percent of cyt c_1 reduced after the flash relative to the total cyt c_1 flash-oxidized by Ru_2D (the initial drop in 552 nm absorbance). nd = not detected.

No electron transfer from reduced [2Fe2S] to photooxidized cyt c_1 was observed at all at pH 6.0, indicating a large negative value for ΔE_0 (Figure 1a). A very small monophasic increase in 552 nm absorbance was observed at pH 7 due to electron transfer from [2Fe2S] to cyt c_1 with a rate constant of 9300 s^{-1} and an amplitude of 5% of the total cyt c_1 photooxidized (the initial decrease in absorbance at 552 nm) (Figure 1b, Table 1). At pH 8, the 552 nm transient due to electron transfer from [2Fe2S] to cyt c_1 was biphasic with an initial fast rate constant, k_{1f}, of 6300 ± 3000 s^{-1} and a slower rate constant, k_{1s}, of 640 ± 300 s^{-1} (Figure 1c, Table 1). The relative amplitudes of k_{1f} and k_{1s} were 10 ± 4% and 16 ± 4%, respectively. The transient could also be adequately fit by the Kohlrausch–Williams–Watts stretched exponential function with the parameters k_1 = 1350 ± 300 s^{-1}, A_1 = 31 ± 6%, and β = 0.44 ± 0.15, shown in Table 3. The electron transfer signal at pH 9 was similar to that at pH 8 (Figure 1d, Table 1).

Electron Transfer between the ISP and Heme c_1 in the Presence of P_m Type Inhibitors. In order to study the effects of P_m type inhibitors on the electron transfer between the ISP and cyt c_1, experiments utilizing the ruthenium flash method described above were conducted in the presence of three P_m inhibitors: MOAS, myxothiazol, and azoxystrobin. Addition of MOAS at pH 6 resulted in a very small monophasic electron transfer transient with a rate constant of 16 000 s^{-1} and amplitude of 5% (Figure 1a, Table 1). In contrast, addition of MOAS at pH 7.0 led to a large biphasic transient with rate constants of 14 000 and 2100 s^{-1} and amplitudes of 40 and 15%, respectively (Figure 1b). At pH 8, MOAS binding led to increases of 3.3-fold and 1.6-fold in the amplitudes of k_{1f} and k_{1s} of the biexponential fit, respectively (Figure 1c, Table 1). The rate constant *k* of the stretched-exponential fit was increased from 1350 to 5200 s^{-1} at pH 8, the β parameter was increased from 0.44 to 0.62, and the amplitude was increased 2-fold (Table 3). Similar effects of MOAS binding were observed at pH 9 (Figure 1d, Table 1).

Addition of 25 μM of the P_m type inhibitor myxothiazol at pH 8 significantly increased the total amplitude of the transient and changed the relative amplitudes of the fast and slow phases (Table 2, Figure 2a). Addition of 25 μM of the P_m inhibitor azoxystrobin had a similar effect on the kinetics of electron transfer from the ISP to cyt c_1 (Table 2, Figure 2b). When fit to the stretched exponential function, both myxothiazol and azoxystrobin increased the rate constant, amplitude, and the value of β as shown in Table 3.

Electron Transfer between the ISP and Heme c_1 in the Presence of P_f Type Inhibitors. Three P_f type inhibitors—stigmatellin, JG-144, and famoxadone—were also used to study the effects on the electron transfer between the ISP and cyt c_1. Stigmatellin, unlike JG-144 and famoxadone, forms a H-bond to His^{161} of the ISP. Addition of 25 μM stigmatellin completely quenched the rereduction of cyt c_1 by the ISP on the time scale of the transient, as shown in Figure 2c, revealing a flat step function. This is consistent with the role of stigmatellin in locking the ISP at the Q_o site via a hydrogen bond to the [2Fe2S] cluster.

JG-144 and famoxadone are both P_f inhibitors, but neither forms a hydrogen bond with the [2Fe2S] His ligand. In the presence of 40 μM JG-144, electron transfer between the ISP and cyt c_1 was biphasic, with a fast rate constant k_{1f} of 1300 s^{-1} and a slow rate constant k_{1s} of 300 s^{-1} (Figure 2d, Table 2). The relative amplitudes of k_{1f} and k_{1s} in the presence of JG-144 were 16% and 29%, respectively (Table 2). A fit of the results following addition of JG-144 to the stretched exponential function showed that the rate constant was decreased ~3-fold to 400 s^{-1}, while the total relative amplitude was increased as shown in Table 3. In the presence of 25 μM famoxadone, the values of k_{1f} and k_{1s} were 600 s^{-1} and 100 s^{-1}, respectively (Figure 2e, Table 2). The relative amplitudes of the two phases k_{1f} and k_{1s} under these conditions were 26% and 20%, respectively, of the total amount of heme c_1 flash oxidized. Thus, both JG-144 and famoxadone decreased the rate constants k_{1f} and k_{1s} and increased their amplitudes.

Electron Transfer between the ISP and Heme c_1 in the Presence of Quinol Substrate. Experiments were also performed using 100 μM decylubiquinone as substrate. In these experiments, 1 mM succinate and 50 nM SCR were added to reduce the quinone pool. Since the amount of

Table 2. Effects of Q_o Site Inhibitors on Electron Transfer in *P. den* cyt bc_1[a]

inhibitor/substrate	type	k_{1f} (s^{-1})	A_{1f} (%)	k_{1s} (s^{-1})	A_{1s} (%)	k_2 (s^{-1})
none		6300 ± 3000	10 ± 3	640 ± 300	16 ± 4	0
MOAS	P_m	9900 ± 2000	33 ± 7	1800 ± 400	26 ± 5	0
myxothiazol	P_m	8900 ± 1800	30 ± 6	1700 ± 300	30 ± 6	0
azoxystrobin	P_m	8000 ± 1600	28 ± 6	1300 ± 1800	24 ± 5	0
stigmatellin	P_f	0	0	0	0	0
JG-144	P_f	1300 ± 300	16 ± 3	300 ± 60	29 ± 6	0
famoxadone	P_f	600 ± 200	26 ± 5	100 ± 20	20 ± 5	0
Q		5300 ± 1100	10 ± 2	500 ± 100	18 ± 5	0
QH_2		10700 ± 2100	18 ± 4	800 ± 200	60 ± 12	700 ± 400

[a]Approximately 5 μM cyt bc_1 was rapidly oxidized by 20 μM Ru_2D following a laser flash in 20 mM TRIS-HCl pH 8.0. 5 mM $[Co(NH_3)_5Cl]^{2+}$ was present to act as a sacrificial oxidant of excited state Ru_2D. Cyt c_1 and [2Fe2S] were reduced by 1 mM ascorbate and 4 μM TMPD. All solutions were purged with an N_2 flush and kept at 10 °C. Experiments with quinol substrate included 100 μM decylubiquinone reduced by 1 mM succinate and 50 nM SCR . All inhibitors were added to 25 μM, except JG-144, which was added to 40 μM. The rate constants k_{1f} and k_{1s} represent the fast and slower phases observed at 552 nm, respectively. A_{1f} and A_{1s} are the respective amplitudes of k_{1f} and k_{1s} and are presented as a percent of the total heme c_1 flash oxidized (the initial drop in 552 nm absorbance). The rate constant k_2 was observed at the cyt c_1 isosbestic, 560 nm, and represents electron transfer to the *b* hemes following turnover in the presence of quinol substrate.

endogenous quinone in the purified samples was approximately two quinones per bc_1 monomer, SCR and succinate were added prior to decylubiquinone as a control. Spectra taken under these conditions show minimal reduction of cyt c_1 or hemes *b* (Figure 3), consistent with the lack of sufficient endogenous quinone to transfer electrons from SCR to purified cyt bc_1. Upon addition of 100 μM decylubiquinone along with 1 mM succinate and 50 nM SCR, cyt c_1 was fully reduced while heme b_H was about 85% reduced (Figure 3). The amplitude of k_{1f} was increased 2-fold by addition of 100 μM decylubiquinol (Table 2, Figure 4a). Following initial oxidation of cyt c_1 and the ISP by the flash, subsequent oxidant-induced reduction of heme b_L and heme b_H was observed at the cyt c_1 isosbestic 560 nm with a rate constant k_2 of 700 s^{-1} (Table 2, Figure 4b). This reaction results from transfer of the first electron from quinol in the Q_o site to the flash-oxidized ISP and cyt c_1, followed by transfer of the second electron from the semiquinone intermediate in the Q_o site to heme b_L and then to heme b_H. This oxidant-induced reduction of the *b* hemes was not observed in the absence of decylubiquinol or the presence of the P_m or P_f inhibitors because there was no ubiquinol in the Q_o site for the reaction.

Flash photolysis experiments were also carried out with the quinone fully oxidized and cyt c_1 and the ISP reduced by ascorbate and TMPD. Addition of the oxidized decylubiquinone decreased the rate constants k_{1f} and k_{1s} to values of 5000 s^{-1} and 500 s^{-1}, respectively (Table 2). However, the amplitudes of these phases were not changed significantly.

DISCUSSION

An important goal toward understanding the mechanism of cyt bc_1 is elucidating the factors that influence the motion of the extrinsic domain of the ISP. The requirement for a mobile ISP domain for electron transfer between the Q_o site and cytochrome c_1 was a surprising discovery arising from the initial crystal structures and has remained the focus of intense research. The controlled motion of the ISP domain may also play a role in a gating mechanism for the electron bifurcation reaction at the Q_o site that is required to prevent short-circuit and bypass reactions.[14,40−45] While the detailed mechanism of controlled domain motion of the ISP remains unclear, it is evident from the crystal structures that the type of inhibitor bound at the Q_o site has an influence on the position and mobility of the ISP. Xia et al. have described the effects of the two different types of Q_o site inhibitors on the position of the ISP.[17,42] Crystal structures complexed with P_m type inhibitors show that the ISP is released from the *b*-state to a disordered state not detected in the crystal, while structures complexed with P_f type inhibitors show that ISP binds to the *b* subunit in a "fixed" state. Berry and Huang[30] have recently analyzed the effects of a wide range of Q_o site inhibitors on the position of the ISP determined by X-ray crystallography. EPR studies have also provided valuable information on the effect of Q_o site inhibitors on the position and orientation of the ISP.[22,27,28,31,32]

We have studied the effects of six different Q_o site inhibitors on the electron transfer reaction from ISP to cyt c_1 in *P. denitrificans* cyt bc_1 following photo-oxidation of cyt c_1 by the excited state of Ru_2D. Three of the inhibitors used in the present study were of the type P_m (MOAS, myxothiazol, and azoxystrobin), and three were of the type P_f (stigmatellin, famoxadone, and JG-144). The effect of MOAS binding was studied as a function of pH to investigate the role of the redox potential difference between the [2Fe2S] center and cyt c_1 in the reaction (Table 1, Figure 1). In the absence of MOAS, there was no electron transfer signal at all at pH 6, indicating a large negative value of $\Delta E_0 = E_0(c_1) - E_0(\text{FeS})$. These results are consistent with the reported redox potentials of +360 and +313 mV for the ISP of *P. denitificans* at pH 6 and 7, respectively,[46] and +211 mV for cyt c_1 at pH 7 (Dr. Petra Hellwig, personal communication). Although no redox potential has been reported for cyt c_1 in *P. den.* cyt bc_1 at pH 6, it has very little pH dependence between pH 6 and pH 7 in *R. sphaeroides* or *R. capsulatus* cyt bc_1.[39] Assuming ΔE_0 = (+211) − (+360) = −0.149 mV at pH 6, the equilibrium constant $K_{eq} = [c_1(\text{red})\text{FeS}(\text{ox})]/[c_1(\text{ox})\text{FeS}(\text{red})]$ is estimated to be 0.003, consistent with the lack of any electron transfer from [2Fe2S] to cyt c_1 at pH 6. This observation also provides additional evidence that Ru_2D does not photooxidize [2Fe2S] directly, since this would result in electron transfer from cyt c_1 to photooxidized [2Fe2S], resulting in a transient decrease in 552 nm absorbance. There is only a small monophasic electron transfer transient at pH 7, with a rate constant of 9300 s^{-1} and an amplitude of 5%, which is consistent with a redox potential difference of ΔE_0 = −77 mV. This value is in reasonable agreement with the ΔE_0 value of −102 mV estimated from the data of ref 46 and Dr. Petra Hellwig (personal communication). At pH 8, electron transfer was biphasic with rate constants k_{1f} of

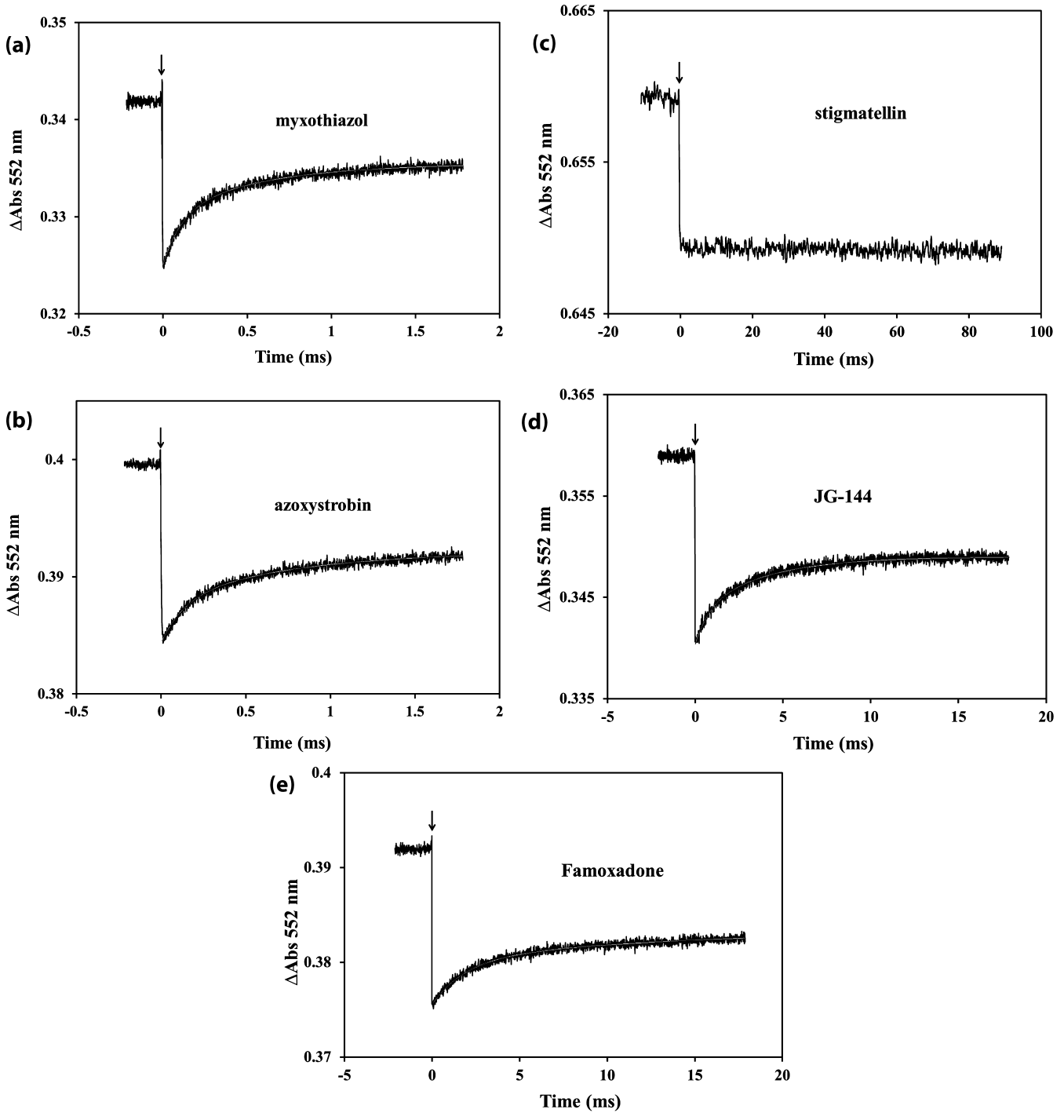

Figure 2. Electron transfer in *P. den* cyt bc_1 in the presence of P_m and P_f type inhibitors Approximately 5 μM cyt bc_1 was rapidly oxidized by 20 μM Ru_2D following laser flash in a 300 μL anaerobic solution of 20 mM TRIS pH 8.0 at 10°C. 5 mM $[Co(NH_3)_5Cl]^{2+}$ was present to act as a sacrificial oxidant of excited state Ru_2D. Cyt c_1 and [2Fe2S] were reduced by 1 mM ascorbate and 4 μM TMPD. P_m inhibitors myxothiazol (a) and azoxystrobin (b) were added to 25 μM. Effects of P_f inhibitors stigmatellin (c, 25 μM), JG-144 (d, 40 μM), and famoxadone (e, 25 μM) are also shown. Note the difference in time scale of the P_f inhibitors compared to the P_m inhibitors. Each transient was fit by the sum of two exponentials represented by the white line, with the kinetic parameters given in Table 2.

6300 ± 3000 s^{-1} and k_{1s} of 640 ± 300 s^{-1} and relative amplitudes of 10 ± 4% and 16 ± 4%, respectively. The transient could also be adequately fit by the Kohlrausch–Williams–Watts stretched exponential function with the parameters k_1 = 1350 ± 300 s^{-1}, A_1 = 31 ± 6%, and β = 0.44 ± 0.15, shown in Table 3. The stretched exponential function represents a continuous distribution of exponentials, where β is inversely related to the Levy distribution of rate constants. The non-monoexponential kinetics indicates that the domain rotation of the ISP has complex dynamics. The total amplitude of 28 ± 4% for electron transfer from the ISP to cyt c_1 is consistent with a redox potential difference ΔE_0 of −24 mV, assuming that all the reduced ISP is able to redox equilibrate with the photooxidized cyt c_1 during the time period of the

dx.doi.org/10.1021/bi200453r | *Biochemistry* 2011, 50, 10462–10472

Table 3. Kohlrausch–Williams–Watts Stretched Exponential Fits[a]

inhibitor/substrate	type	k (s^{-1})	A	β
none		1350 ± 300	31 ± 6	0.44 ± 0.15
MOAS	P_m	5200 ± 1000	62 ± 7	0.62 ± 0.12
myxothiazol	P_m	4100 ± 800	64 ± 6	0.66 ± 0.13
azoxystrobin	P_m	2800 ± 600	53 ± 6	0.63 ± 0.12
stigmatellin	P_f	0	0	0
JG-144	P_f	400 ± 100	43 ± 3	0.74 ± 0.15
famoxadone	P_f	300 ± 100	45 ± 5	0.68 ± 0.14

[a]The transients shown in Figure 2 were also fit by the stretched exponential function, $A = A_1(1 - \exp(-kt)^{\beta})$, where A_1 and k represent the amplitude and rate constant for electron transfer from [2Fe2S] to cyt c_1, respectively, and $0 < \beta < 1$. A_1 is reported as the percent of cyt c_1 reduced after the flash relative to the total cyt c_1 flash-oxidized by Ru_2D. Solution conditions are the same as described in Table 2 and Figure 2.

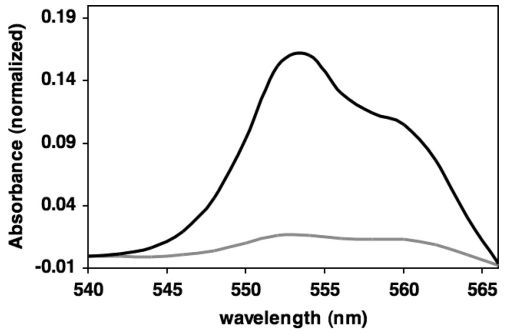

Figure 3. Normalized difference spectra at 540 nm of 7.7 μM *P. den* cyt bc_1 after addition of 1.5 mM succinate and 50 nM SCR (gray) and after subsequent addition of 100 μM decylubiquinone (black). Theoretical fits to the respective difference spectra based on the published difference values of Shinkarev et al.[68] revealed the gray line prior to the addition of substrate to consist of 0.8 μM reduced cyt c_1 and 0.8 μM reduced heme b_H. The black line after addition of substrate revealed that 7.7 μM cyt c_1 and 6.7 μM heme b_H were reduced.

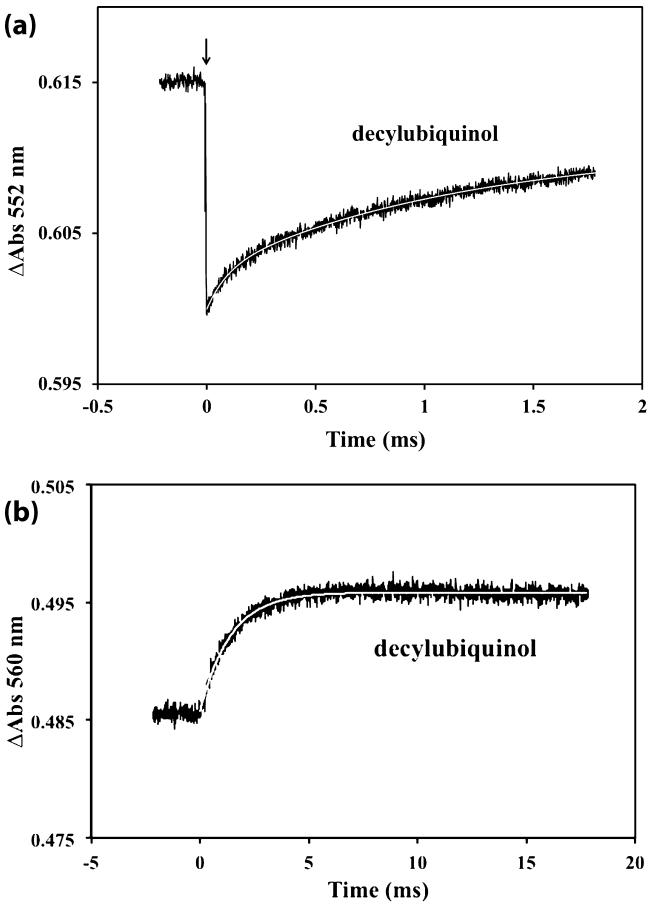

Figure 4. Electron transfer in *P. den* cyt bc_1 in the presence of quinol substrate at 552 nm (a) and 560 nm (b). Approximately 5 μM cyt bc_1 was rapidly oxidized by 20 μM Ru_2D following laser flash in a 300 μL anaerobic solution of 20 mM TRIS pH 8.0 at 10°C. 5 mM $[Co(NH_3)_5Cl]^{2+}$ was present to act as a sacrificial oxidant of excited state Ru_2D. Cyt c_1 and [2Fe2S] were reduced by 1 mM ascorbate and 4 μM TMPD. 100 μM decylubiquinone was added and reduced by the addition of 1 mM succinate and 50 nM SCR. The white line through each transient is an exponential fit. The 552 nm transient was fit by a sum of two exponentials using the values given in Table 2. The 560 nm transient was fit by a single exponential function using the values given in Table 2.

reaction. Although the redox potentials of the ISP and cyt c_1 have not been measured at pH 8.0 in *P. denitrificans*, this small value of ΔE_0 is comparable to that measured in bovine, *R. sphaeroides*, and *R. capsulatus*.[39,47] The kinetics at pH 9 in the absence of inhibitors were similar to those at pH 8.

Binding MOAS to the Q_o site resulted in a small increase in the amplitude of the electron transfer signal at pH 6. Since the value of ΔE_0 is so negative in the absence of MOAS, an increase in ΔE_0 upon MOAS binding would not have a very large effect. In contrast, MOAS binding led to a very large increase in the amplitude of the signal at pH 7.0 (Table 1, Figure 1b). The total change in the amplitude in the signal is consistent with a decrease in the redox potential of the ISP of 82 mV caused by binding MOAS. This is much larger than the decrease of 30 mV observed for the binding of MOAS to *R. capsulatus* cyt bc_1 at pH 7.[48] The conversion from monophasic to biphasic kinetics indicates a complex effect of MOAS binding on the dynamics of ISP domain rotation. MOAS binding also had a significant effect on the kinetics of electron transfer at pH 8. The amplitudes of the fast and slow phases of the biphasic fit increased 3.3-fold and 1.6-fold, respectively, while the rate constant k of the stretched-exponential fit was increased from 1350 to 5200 s^{-1} (Table 1). The total amplitude of the electron transfer signal of 59% is consistent with a difference in redox potential ΔE_0 of 9 mV, which is 33 mV higher than ΔE_0 in the absence of MOAS. A 33 mV decrease in the redox potential of [2Fe2S] upon binding of MOAS is comparable to the value of 30 mV reported for *R. capsulatus* cyt bc_1.[48] Similar results were observed for the effect of MOAS binding at pH 9 (Table 1). Myxothiazol and azoxystrobin were also found to have similar effects to that of MOAS at pH 8 (Table 2). The increase in total amplitude is consistent with the 30 mV decrease in redox potential of [2Fe2S] observed upon binding myxothiazol to *R. capsulatus* cyt bc_1.[27] The kinetic parameters indicate that MOAS, myxothiazol, and azoxystrobin binding have complex effects on the kinetics of electron transfer from ISP to cyt c_1 that go beyond the effects on the redox potential of [2Fe2S]. The increase in k_1 of the stretched-exponential fit and the increase in the ratio of the fast to slow phases of the biexponential fit both indicate a significant change in the dynamics of the ISP. Cooley et al.[31] found that myxothiazol binding to the Q_o site of R. capsulatus cyt bc_1 increased the

dx.doi.org/10.1021/bi200453r | *Biochemistry* 2011, 50, 10462–10472

disorder of the [2Fe2S] center measured by the orientational dependence of the EPR signal. In fact, they proposed that the decrease in redox potential of the ISP is a consequence of the displacement from the *b* state. Sarewicz et al.[32] reported that the average [2Fe2S]−cyt b_L distance is increased upon myxothiazol binding, indicating that the average equilibrium position of [2Fe2S] is moved farther away from the *b* state toward the c_1 state. These EPR studies are in general agreement with the X-ray crystallographic studies showing that myxothiazol and MOAS binding to the Q_o site decreases the occupation of ISP in the *b* state, releasing it to a state not detected by X-ray diffraction.[11,14,16,17] The present studies complement the X-ray crystallographic and EPR studies by providing kinetic information on the rate of rotation of the ISP to the c_1 position. It has been established in *R. sphaeroides* cyt bc_1 that the rate constant k_1 is "conformationally gated" by the rotation of the ISP to the c_1 state where very rapid electron transfer can occur ($k_{et} > 10^6$ s^{-1}).[26]

Addition of the P_f inhibitor stigmatellin completely quenched the rereduction signal at 552 nm, consistent with the formation of a hydrogen bond between the ISP and stigmatellin which completely immobilizes the ISP. In contrast to the effect of stigmatellin, the P_f inhibitors JG-144 and famoxadone decreased the rate constants k_{1f} and k_{1s} by up to 10-fold and increased the amplitudes of these phases up to 2-fold (Table 2, Figure 2d,e). The parameters for the stretched-exponential function following addition of JG-144 and famoxadone show a 3.4-fold decrease in the rate constant and up to a 1.5-fold increase in the relative amplitude. X-ray crystallography studies have indicated that JG-144 and famoxadone binding to the Q_o site displaces the cd1 and *ef* helices outward to form a docking crater which binds the ISP in the *b*-state.[14,30] However, neither JG-144 nor famoxadone interacts directly with the ISP. The present studies indicate that JG-144 or famoxadone binding to the Q_o site of *P. den.* cyt bc_1 does not lock the ISP in the *b* state, but instead decreases the rate of release of the ISP from the *b* state by up to 10-fold. The finding that the amplitudes of the k_{1f} and k_{1s} phases are increased by JG-144 or famoxadone binding suggests that these inhibitors may decrease the redox potential of the ISP. However, no data on the effect of these inhibitors on the ISP redox potential have been published.

Electron transfer within *P. den* cyt bc_1 was also studied in the presence of the ubiquinol substrate decylubiqinol. In the presence of 100 μM decylubiquinone, cyt c_1 in *P. denitrificans* is fully reduced by succinate and SCR, while cyt b_H is 85% reduced. Photo-oxidation of cyt c_1 results in rapid electron transfer from reduced ISP to cyt c_1 with a rate constant k_{1f} of 10 700 s^{-1}, followed by oxidant-induced reduction of cyt b_H with a rate constant k_2 of 700 s^{-1}. This reaction results from transfer of the first electron from quinol in the Q_o site to the flash-oxidized ISP and cyt c_1, followed by transfer of the second electron from the semiquinone intermediate in the Q_o site to heme b_L and then to heme b_H. The amplitude of the initial phase of electron transfer k_{1f} from reduced ISP to photo-oxidized cyt c_1 in the presence of decylubiquinol was 2-fold larger than that of cyt bc_1 reduced by ascorbate and TMPD in the absence of added decylubiquinol substrate (Figure 4a, Table 2). Interestingly, these effects are not observed in the presence of oxidized decylubiquinone, suggesting they are due specifically to the binding of decylubiquinol. Binding oxidized decylubiquinone to cyt bc_1 decreased k_{1f} and k_{1s} but did not affect their amplitudes (Table 2), consistent with the interaction of the reduced ISP with an oxidized quinone in the Q_o pocket.[49−51] These results suggest that decylubiquinol substrate binding to the bc_1 complex affects the conformational dynamics of the reduced ISP in much the same way as the P_m inhibitors do.

The mechanism for bifurcated electron transfer at the Q_o site involving transfer of the first electron from quinol to the ISP and cyt c_1 and the second electron from semiquinone to cyt b_L and cyt b_H has been the subject of intensive research.[40,42,49−57] Any mechanism for this process must account for the reversibility of the reaction as well as the minimization of short-circuit reactions such as the delivery of both electrons from quinol to the high potential chain. Double gating mechanisms have been proposed that require both the ISP and cyt b_L to be oxidized and the ISP in the *b* state in order for quinol to react at the Q_o site.[40,53−57] A Coulombic gating mechanism has been proposed in which the movement of the semiquinone from the distal site near the ISP to a site near oxidized cyt b_L is controlled by electrostatics, thus favoring electron transfer to oxidized cyt b_L and minimizing electron transfer from reduced cyt b_L.[49,55] Concerted mechanisms have been proposed involving simultaneous transfer of two electrons from quinol to the ISP and cyt b_L without the formation of a semiquinone intermediate.[40,54,56−58] However, two different groups have recently detected a semiquinone radical at the Q_o site,[59,60] and the bypass reaction involving formation of superoxide is also thought to require a semiquinone.[61]

Structural linkages between the quinol substrate in the Q_o binding site and the conformation of the ISP have been proposed to play a role in the mechanism of bifurcated electron transfer.[17,42] Although it has not been possible to experimentally detect QH_2 or Q in the Q_o binding pocket, the effects of Q_o site inhibitors on the linked conformations of cyt *b* and the ISP have led to a proposal for the role of ISP domain orientation in bifurcated electron transfer.[17,42] Binding QH_2 to the Q_o site would move the cd1 and *ef* helices outward and bind the oxidized ISP in the docking crater in the *b* state. Formation of a hydrogen bond between QH_2 and His-161 would lead to proton-coupled electron transfer from QH_2 to oxidized [2Fe2S]. Following transfer of the second electron from semiquinone to cyt b_L and cyt b_H, oxidized Q would leave the distal Q_o binding pocket, allowing the cd1 and *ef* helices to come closer together and release the ISP from the docking crater so it could rotate to the c_1 position and transfer an electron to cyt c_1.[17,42] The effects of the P_m and P_f inhibitors on the kinetics of *P. denitiricans* cyt bc_1 are consistent with this proposal and provide additional evidence that the conformations of the Q_o site, the ISP binding crater, and the ISP domain orientation are tightly linked. Binding P_f inhibitors to the Q_o site would lead to a conformation similar to that of the active QH_2-oxidized ISP complex, while binding P_m inhibitors would lead to a conformation in which the ISP is released from the *b* state to a mobile state. These studies provide additional evidence that binding orientations of QH_2 and the ISP are tightly linked by the Q_o site and ISP binding crater conformations on cyt *b*. This linkage may play an important role in gating the electron transfer bifurcation reaction in the Q_o site to minimize short-circuit and bypass reactions. It is likely that other factors are also involved in gating, such as Coulombic gating of the motion of the semiquinone[49,55] and the conformations of water or amino acid side chains in the Q_o pocket.[40,53−57] A number of studies have suggested that events at the Q_i site and the b_L and b_H hemes might also be linked to turnover at the Q_o site.[31,32,45,62−66]

In conclusion, the present studies show that the species occupying the Q_o site of *P. den* cyt bc_1 influences the kinetics of domain rotation of the ISP between the *b* state and the c_1 state. In the presence of oxidized quinone, the rate and amplitude of electron transfer from ISP to cyt c_1 are small, consistent with an interaction between quinone and the reduced ISP. Addition of the P_m inhibitors increases the rate and extent of electron transfer from ISP to cyt c_1, consistent with release from the b state which causes a linked decrease in the redox potential and increase in the mobility of the ISP. Addition of the P_f inhibitors JG-144 or famoxadone substantially decreases the rate of release to the mobile state. Binding reduced QH_2 leads to release of reduced ISP from the *b* state to the mobile state, allowing electron transfer to cyt c_1. The reaction of *P. denitiricans* cyt bc_1 with its native substrate cytochrome c_{552} has been described in a recent publication.[67]

■ ASSOCIATED CONTENT

Ⓢ Supporting Information

Three figures providing data about the mechanism of photooxidation of cyt c_1 by Ru_2D. This material is available free of charge via the Internet at http://pubs.acs.org.

■ AUTHOR INFORMATION

Corresponding Author

*Phone: 479-575-4999. Fax: 479-575-4049. E-mail: millett@uark.edu.

Author Contributions

[§]J.H. and M.C. contributed equally to this work.

Present Addresses

[∥]Department of Molecular Membrane Biology, Max Planck Institute for Biophysics, Max-von-Laue Strasse 3 60438 Frankfurt am Main

[⊥]Institute for Biochemistry and Molecular Biology, ZMBZ, BIOSS Centre for Biological Signaling Studies, Stefan-Meier-Strasse 17, Albert-Ludwigs-University, 79104 Freiburg, Germany

Funding

This work was supported in part by NIH grants GM20488 and NCRR COBRE 5P30RR031154. The Collaborative Research Center "Molecular Bioenergetics" (SFB 472), the Center for Membrane Proteomics (CMP), and the Cluster of Excellence Frankfurt (Macromolecular Complexes, DFG Project EXC 115) are acknowledged for financial support.

■ ACKNOWLEDGMENTS

We thank Drs. Petra Hellwig and Youssef El Khoury (University of Strasbourg) for determination of the endogenous quinone substrate content of purified cytochrome bc_1.

■ ABBREVIATIONS

Cc, cytochrome *c*; cyt bc_1, cytochrome bc_1; ET, electron transfer; FP, flash photolysis; ISP, Rieske iron−sulfur protein; [2Fe2S], iron−sulfur center of ISP; MOAS, methoxyacrylate stilbene; *P. den*, *P. denitrificans*; Ru_2D, $[Ru(bpy)_2]_2(qpy)(PF_6)_4$; qpy, 2,2′:4′,4″:2″,2‴-quaterpyridine; SCR, succinate−cytochrome *c* reductase; DDM, dodecylmaltoside; TMPD, *N*,*N*,*N*′,*N*′-tetramethyl-*p*-phenylenediamine.

■ REFERENCES

(1) Trumpower, B. L., and Gennis, R. B. (1994) Energy transduction by cytochrome complexes in mitochondrial and bacterial respiration: the enzymology of coupling electron transfer reactions to transmembrane proton translocation. *Annu. Rev. Biochem. 63*, 675−716.

(2) Trumpower, B. L. (1990) The protonmotive Q cycle. Energy transduction by coupling of proton translocation to electron transfer by the cytochrome bc_1 complex. *J. Biol. Chem. 265*, 11409−11412.

(3) Kurowski, B., and Ludwig, B. (1987) The genes of the Paracoccus denitrificans bc_1 complex. Nucleotide sequence and homologies between bacterial and mitochondrial subunits. *J. Biol. Chem. 262*, 13805−13811.

(4) Kim, C. H., Balny, C., and King, T. E. (1987) Role of the hinge protein in the electron transfer between cardiac cytochrome c_1 and *c*. Equilibrium constants and kinetic probes. *J. Biol. Chem. 262*, 8103−8108.

(5) Schmitt, M. E., and Trumpower, B. L. (1990) Subunit 6 regulates half-of-the-sites reactivity of the dimeric cytochrome bc_1 complex in Saccharomyces cerevisiae. *J. Biol. Chem. 265*, 17005−17011.

(6) Morgner, N., Kleinschroth, T., Barth, H. D., Ludwig, B., and Brutschy, B. (2007) A novel approach to analyze membrane proteins by laser mass spectrometry: from protein subunits to the integral complex. *J. Am. Soc. Mass Spectrom. 18*, 1429−1438.

(7) Mitchell, P. (1975) The protonmotive Q cycle: a general formulation. *FEBS Lett. 59*, 137−139.

(8) Crofts, A. R. (2004) The cytochrome bc_1 complex: function in the context of structure. *Annu. Rev. Physiol. 66*, 689−733.

(9) Xia, D., Yu, C. A., Kim, H., Xia, J. Z., Kachurin, A. M., Zhang, L., Yu, L., and Deisenhofer, J. (1997) Crystal structure of the cytochrome bc_1 complex from bovine heart mitochondria. *Science 277*, 60−66.

(10) Zhang, Z., Huang, L., Shulmeister, V. M., Chi, Y. I., Kim, K. K., Hung, L. W., Crofts, A. R., Berry, E. A., and Kim, S. H. (1998) Electron transfer by domain movement in cytochrome bc_1. *Nature 392*, 677−684.

(11) Iwata, S., Lee, J. W., Okada, K., Lee, J. K., Iwata, M., Rasmussen, B., Link, T. A., Ramaswamy, S., and Jap, B. K. (1998) Complete structure of the 11-subunit bovine mitochondrial cytochrome bc_1 complex. *Science 281*, 64−71.

(12) Kim, H., Xia, D., Yu, C. A., Xia, J. Z., Kachurin, A. M., Zhang, L., Yu, L., and Deisenhofer, J. (1998) Inhibitor binding changes domain mobility in the iron-sulfur protein of the mitochondrial bc_1 complex from bovine heart. *Proc. Natl. Acad. Sci. U. S. A. 95*, 8026−8033.

(13) Ritter, M., Palsdottir, H., Abe, M., Mäntele, W., Hunte, C., Miyoshi, H., and Hellwig, P. (2004) Direct evidence for the interaction of stigmatellin with a protonated acidic group in the bc_1 complex from Saccharomyces cerevisiae as monitored by FTIR difference spectroscopy and 13C specific labeling. *Biochemistry 43*, 8439−8446.

(14) Esser, L., Quinn, B., Li, Y. F., Zhang, M., Elberry, M., Yu, L., Yu, C. A., and Xia, D. (2004) Crystallographic studies of quinol oxidation site inhibitors: a modified classification of inhibitors for the cytochrome bc_1 complex. *J. Mol. Biol. 341*, 281−302.

(15) Lancaster, C. R., Hunte, C., Kelley, J., Trumpower, B. L., and Ditchfield, R. (2007) A comparison of stigmatellin conformations, free and bound to the photosynthetic reaction center and the cytochrome bc_1 complex. *J. Mol. Biol. 368*, 197−208.

(16) Esser, L., Elberry, M., Zhou, F., Yu, C. A., Yu, L., and Xia, D. (2008) Inhibitor-complexed structures of the cytochrome bc_1 from the photosynthetic bacterium Rhodobacter sphaeroides. *J. Biol. Chem. 283*, 2846−2857.

(17) Xia, D., Esser, L., Yu, L., and Yu, C. A. (2007) Structural basis for the mechanism of electron bifurcation at the quinol oxidation site of the cytochrome bc_1 complex. *Photosyn. Res. 92*, 17−34.

(18) Sadoski, R. C., Engstrom, G., Tian, H., Zhang, L., Yu, C. A., Yu, L., Durham, B., and Millett, F. (2000) Use of a photoactivated ruthenium dimer complex to measure electron transfer between the Rieske iron-sulfur protein and cytochrome c_1 in the cytochrome bc_1 complex. *Biochemistry 39*, 4231−4236.

(19) Tian, H., Yu, L., Mather, M. W., and Yu, C. A. (1998) Flexibility of the neck region of the rieske iron-sulfur protein is functionally important in the cytochrome bc_1 complex. *J. Biol. Chem. 273*, 27953−27959.

(20) Xiao, K., Yu, L., and Yu, C. A. (2000) Confirmation of the involvement of protein domain movement during the catalytic cycle of the cytochrome bc_1 complex by the formation of an intersubunit

disulfide bond between cytochrome *b* and the iron-sulfur protein. *J. Biol. Chem. 275*, 38597−38604.
(21) Tian, H., White, S., Yu, L., and Yu, C. A. (1999) Evidence for the head domain movement of the rieske iron-sulfur protein in electron transfer reaction of the cytochrome bc_1 complex. *J. Biol. Chem. 274*, 7146−7152.
(22) Darrouzet, E., Valkova-Valchanova, M., and Daldal, F. (2000) Probing the role of the Fe-S subunit hinge region during Q_o site catalysis in Rhodobacter capsulatus bc_1 complex. *Biochemistry 39*, 15475−15483.
(23) Darrouzet, E., Valkova-Valchanova, M., Moser, C. C., Dutton, P. L., and Daldal, F. (2000) Uncovering the [2Fe2S] domain movement in cytochrome bc_1 and its implications for energy conversion. *Proc. Natl. Acad. Sci. U. S. A. 97*, 4567−4572.
(24) Nett, J. H., Hunte, C., and Trumpower, B. L. (2000) Changes to the length of the flexible linker region of the Rieske protein impair the interaction of ubiquinol with the cytochrome bc_1 complex. *Eur. J. Biochem. 267*, 5777−5782.
(25) Ghosh, M., Wang, Y., Ebert, C. E., Vadlamuri, S., and Beattie, D. S. (2001) Substituting leucine for alanine-86 in the tether region of the iron-sulfur protein of the cytochrome bc_1 complex affects the mobility of the [2Fe2S] domain. *Biochemistry 40*, 327−335.
(26) Engstrom, G., Xiao, K., Yu, C. A., Yu, L., Durham, B., and Millett, F. (2002) Photoinduced electron transfer between the Rieske iron-sulfur protein and cytochrome c_1 in the Rhodobacter sphaeroides cytochrome bc_1 complex. Effects of pH, temperature, and driving force. *J. Biol. Chem. 277*, 31072−31078.
(27) Darrouzet, E., Valkova-Valchanova, M., and Daldal, F. (2002) The [2Fe-2S] cluster E_m as an indicator of the iron-sulfur subunit position in the ubihydroquinone oxidation site of the cytochrome bc_1 complex. *J. Biol. Chem. 277*, 3464−3470.
(28) Darrouzet, E., and Daldal, F. (2002) Movement of the iron-sulfur subunit beyond the ef loop of cytochrome *b* is required for multiple turnovers of the bc_1 complex but not for single turnover Q_o site catalysis. *J. Biol. Chem. 277*, 3471−3476.
(29) Brugna, M., Rodgers, S., Schricker, A., Montoya, G., Kazmeier, M., Nitschke, W., and Sinning, I. (2000) A spectroscopic method for observing the domain movement of the Rieske iron-sulfur protein. *Proc. Natl. Acad. Sci. U. S. A. 97*, 2069−2074.
(30) Berry, E. A., and Huang, L. S. (2011) Conformationally linked interaction in the cytochrome bc(1) complex between inhibitors of the Q(o) site and the Rieske iron-sulfur protein. *Biochim. Biophys. Acta 1807*, 1349−1363.
(31) Cooley, J. W., Roberts, A. G., Bowman, M. K., Kramer, D. M., and Daldal, F. (2004) The raised midpoint potential of the [2Fe2S] cluster of cytochrome bc1 is mediated by both the Qo site occupants and the head domain position of the Fe-S protein subunit. *Biochemistry 43*, 2217−2227.
(32) Sarewicz, M., Dutka, M., Froncisz, W., and Osyczka, A. (2009) Magnetic interactions sense changes in distance between heme b(L) and the iron-sulfur cluster in cytochrome bc(1). *Biochemistry 48*, 5708−5720.
(33) Xiao, K., Engstrom, G., Rajagukguk, S., Yu, C. A., Yu, L., Durham, B., and Millett, F. (2003) Effect of famoxadone on photoinduced electron transfer between the iron-sulfur center and cytochrome c_1 in the cytochrome bc_1 complex. *J. Biol. Chem. 278*, 11419−11426.
(34) Millett, F., and Durham, B. (2004) Kinetics of Electron Transfer within Cytochrome bc_1 and Between Cytochrome bc_1 and Cytochrome *c*. *Photosynth. Res. 82*, 1−16.
(35) Engstrom, G., Rajagukguk, R., Saunders, A. J., Patel, C. N., Rajagukguk, S., Merbitz-Zahradnik, T., Xiao, K., Pielak, G. J., Trumpower, B. L., Yu, C. A., Yu, L., Durham, B., and Millett, F. (2003) Design of a ruthenium-labeled cytochrome c derivative to study electron transfer with the cytochrome bc_1 complex. *Biochemistry 42*, 2816−2824.
(36) Rajagukguk, S., Yang, S., Yu, C. A., Yu, L., Durham, B., and Millett, F. (2007) Effect of mutations in the cytochrome *b* ef loop on the electron-transfer reactions of the Rieske iron-sulfur protein in the cytochrome bc_1 complex. *Biochemistry 46*, 1791−1798.
(37) Heacock, D. H., Liu, R. Q., Yu, C. A., Yu, L., Durham, B., and Millett, F. (1993) Intracomplex electron transfer between ruthenium-cytochrome *c* derivatives and cytochrome c_1. *J. Biol. Chem. 268*, 27171−27175.
(38) Williams, G., and Watts, D. C. (1970) Non-symmetrical dielectric relaxation behaviour arising from a simple empirical decay function. *Trans. Faraday Soc. 66*, 80−85.
(39) Zhang, H., Chobot, S. E., Osyczka, A., Wraight, C. A., Dutton, P. L., and Moser, C. C. (2008) Quinone and non-quinone redox couples in Complex III. *J. Bioenerg. Biomembr. 40*, 493−499.
(40) Osyczka, A., Moser, C. C., Daldal, F., and Dutton, P. L. (2004) Reversible redox energy coupling in electron transfer chains. *Nature 427*, 607−612.
(41) Chobot, S. E., Zhang, H., Moser, C. C., and Dutton, P. L. (2008) Breaking the Q-cycle: finding new ways to study Q_o through thermodynamic manipulations. *J. Bioenerg. Biomembr. 40*, 501−507.
(42) Esser, L., Gong, X., Yang, S., Yu, L., Yu, C. A., and Xia, D. (2006) Surface-modulated motion switch: capture and release of iron-sulfur protein in the cytochrome bc_1 complex. *Proc. Natl. Acad. Sci. U. S. A. 103*, 13045−13050.
(43) Yu, C. A., Cen, X., Ma, H. W., Yin, Y., Yu, L., Esser, L., and Xia, D. (2008) Domain conformational switch of the iron-sulfur protein in cytochrome bc_1 complex is induced by the electron transfer from cytochrome b_L to bH. *Biochim. Biophys. Acta 1777*, 1038−1043.
(44) Gurung, B., Yu, L., Xia, D., and Yu, C. A. (2005) The iron-sulfur cluster of the Rieske iron-sulfur protein functions as a proton-exiting gate in the cytochrome bc_1 complex. *J. Biol. Chem. 280*, 24895−24902.
(45) Covian, R., and Trumpower, B. L. (2008) Regulatory interactions in the dimeric cytochrome bc_1 complex: the advantages of being a twin. *Biochim. Biophys. Acta 1777*, 1079−1091.
(46) Schröter, T., Hatzfeld, O. M., Gemeinhardt, S., Korn, M., Friedrich, T., Ludwig, B., and Link, T. A. (1998) Mutational analysis of residues forming hydrogen bonds in the Rieske [2Fe-2S] cluster of the cytochrome bc1 complex in Paracoccus denitrificans. *Eur. J. Biochem. 255*, 100−106.
(47) Zhang, L., Tai, C. H., Yu, L., and Yu, C. A. (2000) pH-induced intramolecular electron transfer between the iron-sulfur protein and cytochrome c_1 in bovine cytochrome bc_1 complex. *J. Biol. Chem. 275*, 7656−7661.
(48) Sharp, R. E., Gibney, B. R., Palmitessa, A., White, J. L., Dixon, J. A., Moser, C. C., Daldal, F., and Dutton, P. L. (1999) Effect of inhibitors on the ubiquinone binding capacity of the primary energy conversion site in the Rhodobacter capsulatus cytochrome bc(1) complex. *Biochemistry 38*, 14973−14980.
(49) Hong, S., Ugulava, N., Guergova-Kuras, M., and Crofts, A. R. (1999) The energy landscape for ubihydroquinone oxidation at the Q_o site of the bc_1 complex in Rhodobacter sphaeroides. *J. Biol. Chem. 274*, 33931−33944.
(50) Crofts, A. R., Hong, S., Zhang, Z., and Berry, E. A. (1999) Physicochemical aspects of the movement of the Rieske iron sulfur protein during quinol oxidation by the bc_1 complex from mitochondria and photosynthetic bacteria. *Biochemistry 38*, 15827−15839.
(51) Lhee, S., Kolling, D., Nair, S., Dikanov, S., and Crofts, A. (2010) Modifications of protein environment of the [2Fe-2S] cluster of the bc_1 complex: Effects on the biophysical properties of the Rieske iron-sulfur protein and on the kinetics of the complex. *J. Biol. Chem. 285*, 9233−9248.
(52) Darrouzet, E., and Daldal, F. (2003) Protein-protein interactions between cytochrome *b* and the Fe-S protein subunits during QH_2 oxidation and large-scale domain movement in the bc_1 complex. *Biochemistry 42*, 1499−1507.
(53) Rich, P. R. (2004) The quinone chemistry of *bc* complexes. *Biochim. Biophys. Acta 1658*, 165−171.
(54) Osyczka, A., Moser, C. C., and Dutton, P. L. (2005) Fixing the Q cycle. *Trends Biochem. Sci. 30*, 176−182.

(55) Crofts, A. R., Lhee, S., Crofts, S. B., Cheng, J., and Rose, S. (2006) Proton pumping in the bc_1 complex: a new gating mechanism that prevents short circuits. *Biochim. Biophys. Acta 1757*, 1019−1034.
(56) Mulkidjanian, A. Y. (2005) Ubiquinol oxidation in the cytochrome bc_1 complex: reaction mechanism and prevention of short-circuiting. *Biochim. Biophys. Acta 1709*, 5−34.
(57) Osyczka, A., Zhang, H., Mathé, C., Rich, P. R., Moser, C. C., and Dutton, P. L. (2006) Role of the PEWY glutamate in hydroquinone-quinone oxidation-reduction catalysis in the Q_o Site of cytochrome bc_1. *Biochemistry 45*, 10492−10503.
(58) Zhu, J., Egawa, T., Yeh, S. R., Yu, L., and Yu, C. A. (2007) Simultaneous reduction of iron-sulfur protein and cytochrome b_L during ubiquinol oxidation in cytochrome bc_1 complex. *Proc. Natl. Acad. Sci. U. S. A. 104*, 4864−4869.
(59) Cape, J. L., Bowman, M. K., and Kramer, D. M. (2007) A semiquinone intermediate generated at the Q_o site of the cytochrome bc_1 complex: importance for the Q-cycle and superoxide production. *Proc. Natl. Acad. Sci. U. S. A. 104*, 7887−7892.
(60) Zhang, H., Osyczka, A., Dutton, P. L., and Moser, C. C. (2007) Exposing the complex III Q_o semiquinone radical. *Biochim. Biophys. Acta 1767*, 883−887.
(61) Forquer, I., Covian, R., Bowman, M. K., Trumpower, B. L., and Kramer, D. M. (2006) Similar transition states mediate the Q-cycle and superoxide production by the cytochrome bc_1 complex. *J. Biol. Chem. 281*, 38459−38465.
(62) Castellani, M., Covian, R., Kleinschroth, T., Anderka, O., Ludwig, B., and Trumpower, B. (2010) Direct Demonstration of Half-of-the-sites Reactivity in the Dimeric Cytochrome bc_1 Complex: Enzyme with one inactive monomer is fully active but unable to activate the second ubiquinol oxidation site in response to ligand binding at the ubiquinone reduction site. *J. Biol. Chem. 285*, 502−510.
(63) Cooley, J. (2010) A structural model for across membrane coupling between the Q_o and Q_i active sites of cytochrome bc_1. *Biochim. Biophys. Acta, Bioenerg. 1797*, 1842−1848.
(64) Mulkidjanian, A. Y. (2007) Proton translocation by the cytochrome bc_1 complexes of phototrophic bacteria: introducing the activated Q-cycle. *Photochem. Photobiol. Sci. 6*, 19−34.
(65) Cen, X., Yu, L., and Yu, C. A. (2008) Domain movement of iron sulfur protein in cytochrome bc_1 complex is facilitated by the electron transfer from cytochrome b_L to b_H. *FEBS Lett. 582*, 523−526.
(66) Lanciano, P., Lee, D. W., Yang, H., Darrouzet, E., and Daldal, F. (2011) Intermonomer electron transfer between the low-potential b hemes of cytochrome bc_1. *Biochemistry 50*, 1651−1663.
(67) Castellani, M., Havens, J., Kleinschroth, T., Millett, F., Durham, B., Malatesta, F., and Ludwig, B. (2011) The acidic domain of cytochrome c_1 in Paracoccus denitrificans, analogous to the acidic subunits in eukaryotic bc_1 complexes, is not involved in the electron transfer reaction to its native substrate cytochrome c_{552}. *Biochim. Biophys. Acta 1807*, 1383−1389.
(68) Shinkarev, V. P., Crofts, A. R., and Wraight, C. A. (2006) Spectral analysis of the bc_1 complex components in situ: beyond the traditional difference approach. *Biochim. Biophys. Acta 1757*, 67−77.